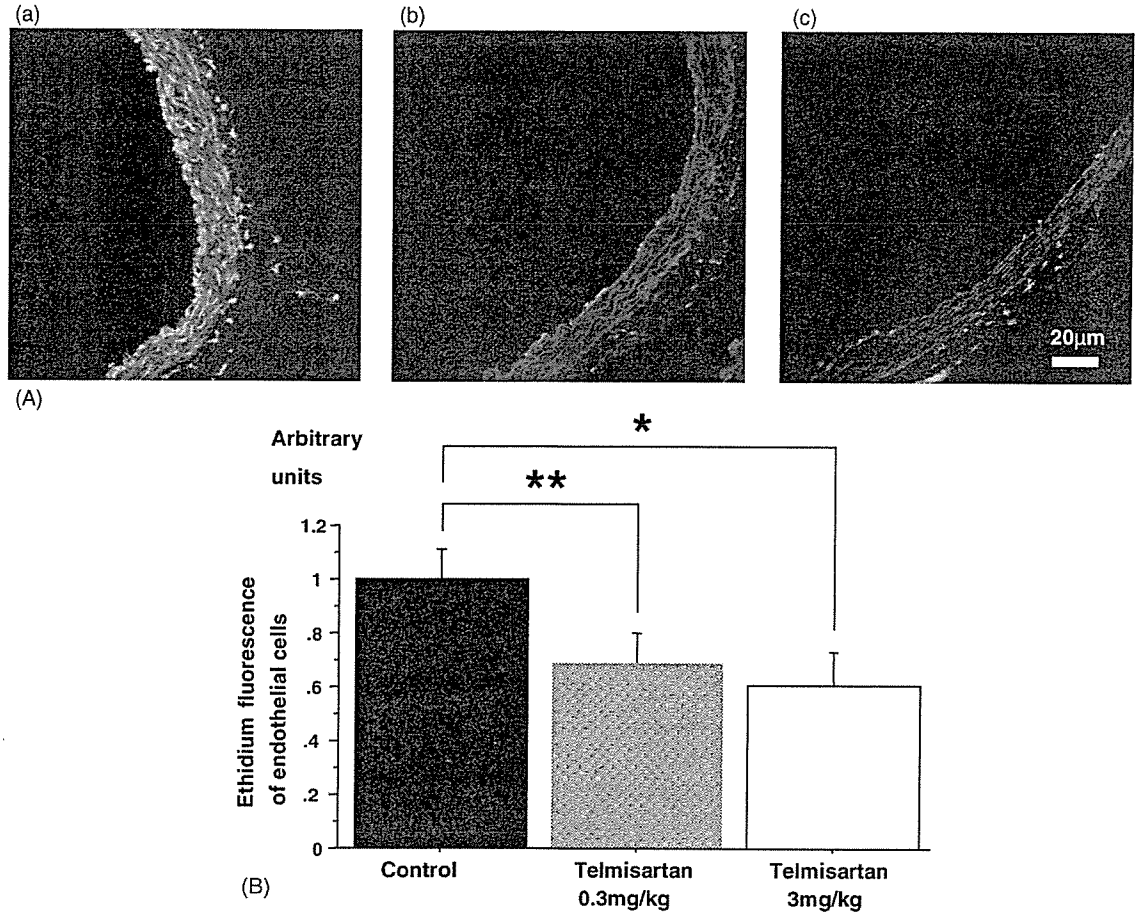

Fig. 4. (A) Representative photographs of in situ superoxide production in aortic vessel wall using dihydroethidium staining. Panel (a) through (c) are representative photographs of aortic vessel wall from each mouse in control group (a), that treated with 0.3 mg/kg telmisartan (b) and that treated with 3 mg/kg telmisartan (c), respectively. Sections were stained with dihydroethidium as described in Section 2. Original magnification were 200×. A white bar represents 20 μm. (B) Quantitative analysis of in situ superoxide production in aorta endothelial cells using dihydroethidium staining. For quantification of ethidium fluorescence from the endothelial cells in high-power (200×) images, fluorescence (intensity × area) was measured only on the luminal side of the internal elastic lamina using the Image J as described in Section 2 and expressed in arbitrary units. Results were expressed as mean ± S.E.M. in each group ($n = 10$ per group). $^{*}P < 0.05$ vs. control; $^{**}P = 0.07$ vs. control.

II-signaling system [21]. Ang II-mediated hypertension is associated with the increased superoxide production and NAD(P)H oxidase activity [7]. Other than hypertension, the increased superoxide production due to NAD(P)H oxidase activation was demonstrated in the rabbit model of atherosclerosis [22]. We examined lucigenin-enhanced CL with NAD(P)H as the substrates and revealed that telmisartan suppressed NAD(P)H dependent oxidase activity with the dosage that did not change blood pressure. This effect was reduced by DPI, an inhibitor of all flavoenzymes and also by apocynin, a more specific inhibitor for NAD(P)H oxidase. These results indicated that the increment of superoxide production was reduced by inactivation of NAD(P)H dependent oxidase activity due to Ang II type 1 receptor blockade with telmisartan.

Our findings are in accordance with the study of Warnholtz et al., who showed that Bay 10-6734, an ARB, reduced plaque formation in association with reductions of vascular superoxide production and NAD(P)H oxidase activity in the rabbit model of atherosclerosis [22]. They did not show whether the anti-atherogenic effects of Bay 10-6734 were independent of the blood pressure lowering effect. In the present study, we clearly demonstrated that telmisartan, a clinically used ARB, reduced atherosclerotic lesion formation without changing blood pressure in apoE-KO mice. In most animal studies showing the blood pressure-independent anti-atherogenic actions of ARB, the far-high dosages have been used compared with those applied clinically [10–13]. In the present study, we showed that the anti-atherogenic action of telmisartan was detected with 0.3 mg/kg, which is lower than the clinically relevant dose. We also showed that telmisartan reduced not only vascular superoxide production but also the marker of systemic oxidative status. 8-*iso*-PGF2α has been recognized as a marker of systemic oxidative stress [23] and revealed as a risk marker in patients with coronary heart disease in matched case-control studies [24]. In this study, telmisartan suppressed 8-*iso*-PGF2α levels in both urine and plasma with the non-blood pressure lowing dosage.

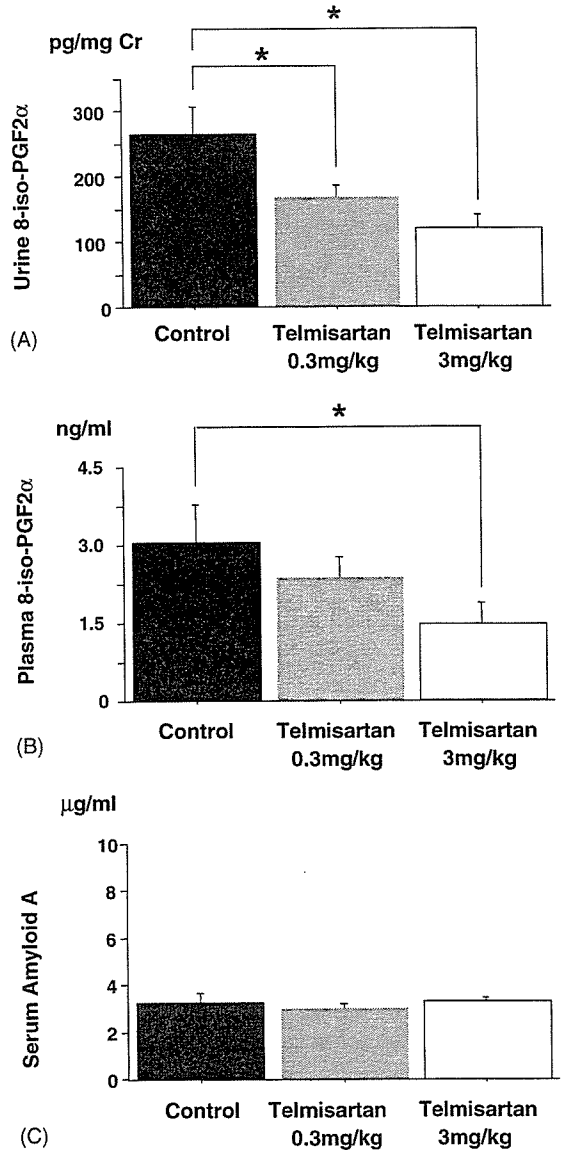

Fig. 5. (A) and (B) Effect of telmisartan on 8-*iso*-PGF2α levels of urine and plasma samples 8-*iso*-PGF2α from urine (A) and plasma (B) samples were measured as described in Section 2. Urine data are corrected by urine creatinine levels. Results were expressed as mean ± S.E.M. ($n = 8$ per group). $^{*}P < 0.05$ vs. control. (C) Effect of telmisartan on SAA levels. SAA levels were measured as described in Section 2. Results were expressed as mean ± S.E.M. ($n = 8$ per group).

The association of suppressed oxidative stress and reduction of atherosclerotic lesion formation does not necessarily mean the cause-effect relation. Both occurred independently of changes in blood pressure, and the well-known roles of oxidative stress in the initiation and progression of atherosclerosis strongly suggest that the anti-oxidative effects are at least partly responsible for the suppression of atherosclerotic lesion formation by telmisartan. Telmisartan might, however, reduce atherosclerotic lesion size by mechanisms other than its effects on oxidative stress, such as anti-inflammatory effects and effects on peroxisome proliferator-activated receptor-gamma (PPAR-g) activity. It is reported that telmisartan induced PPAR-g activation [25,26], but in the present study, telmisartan did not change plasma glucose, triglyceride or insulin levels. Therefore the effect of telmisartan on PPAR-g seemed to play a minimum role in the present study. Further, Ang II increases expression of lectin-like oxidized LDL receptor of macrophage and accelerates the foam cell formation and the deposition of oxidized lipid to the plaque [27]. Further studies are needed to clarify how inhibition of those actions of Ang II by telmisartan is related to its anti-atherogenic action.

As a limitation of the present study, we quantified superoxide production from aorta homogenates by use of 250 μm lucigenin. The validity of data on superoxide has been questioned when the relatively high dose of lucigenin is applied. In the present study, however, the levels of oxidative stress were relatively low, and we could not detect any fluorescence signals when we used 5 μm lucigenin, which was revealed not to produce superoxide by itself. In the report of Warnholtz et al., they compared the data on superoxide productions measured by 5 μM lucigenin with those by 250 μM lucigenin and confirmed the validity of the data obtained by the latter concentration [22].

In conclusion, we for the first time reported that in apoE-KO mice clinically relevant doses of telmisartan reduced atherosclerosis in association with suppressions in vascular oxidative stress and vascular systemic oxidative state. Our results suggest that telmisartan is beneficial not only for hypertension but also for atherosclerosis and imply that this drug may work as an anti-oxidant in various organs, although additional experiments will be needed.

References

[1] Daugherty A, Cassis L. Chronic angiotensin II infusion promotes atherogenesis in low density lipoprotein receptor −/− mice. Ann NY Acad Sci 1999;892:108–18.
[2] Zhang H, Schmeisser A, Garlichs CD, et al. Angiotensin II-induced superoxide anion generation in human vascular endothelial cells: role of membrane-bound NADH/NADPH-oxidases. Cardiovasc Res 1999;44:215–22.
[3] Sorescu D, Weiss D, Lassegue B, et al. Superoxide production and expression of nox family proteins in human atherosclerosis. Circulation 2002;105:1429–35.
[4] Cathcart MK. Regulation of superoxide anion production by NADPH oxidase in monocytes/macrophages: contributions to atherosclerosis. Arterioscler Thromb Vasc Biol 2004;24:23–8.
[5] Diet F, Pratt RE, Berry GJ, Momose N, Gibbons GH, Dzau VJ. Increased accumulation of tissue ACE in human atherosclerotic coronary artery disease. Circulation 1996;94:2756–67.
[6] Yang BC, Phillips MI, Mohuczy D, et al. Increased angiotensin II type 1 receptor expression in hypercholesterolemic atherosclerosis in rabbits. Arterioscler Thromb Vasc Biol 1998;18:1433–9.
[7] Rajagopalan S, Kurz S, Munzel T, et al. Angiotensin II-mediated hypertension in the rat increases vascular superoxide production via membrane NADH/NADPH oxidase activation. Contribution to alterations of vasomotor tone. J Clin Invest 1996;97:1916–23.
[8] Chen XL, Tummala PE, Olbrych MT, Alexander RW, Medford RM. Angiotensin II induces monocyte chemoattractant protein-1 gene expression in rat vascular smooth muscle cells. Circ Res 1998;83:952–9.

[9] Tummala PE, Chen XL, Sundell CL, et al. Angiotensin II induces vascular cell adhesion molecule-1 expression in rat vasculature: a potential link between the renin-angiotensin system and atherosclerosis. Circulation 1999;100:1223–9.
[10] Strawn WB, Chappell MC, Dean RH, Kivlighn S, Ferrario CM. Inhibition of early atherogenesis by losartan in monkeys with diet-induced hypercholesterolemia. Circulation 2000;101:1586–93.
[11] Hayek T, Attias J, Coleman R, et al. The angiotensin-converting enzyme inhibitor, fosinopril, and the angiotensin II receptor antagonist, losartan, inhibit LDL oxidation and attenuate atherosclerosis independent of lowering blood pressure in apolipoprotein E-deficient mice. Cardiovasc Res 1999;44:579–87.
[12] Dol F, Martin G, Staels B, et al. Angiotensin AT1 receptor antagonist in apolipoprotein E-deficient mice. J Cardiovasc Pharmacol 2001;38:395–405.
[13] Takai S, Kim S, Sakonjo H, Miyazaki M. Mechanisms of angiotensin II type 1 receptor blocker for anti-atherosclerotic effect in monkeys fed a high-cholesterol diet. J Hypertens 2003;21:361–9.
[14] Paigen B, Morrow A, Holmes PA, Mitchell D, Williams RA. Quantitative assessment of atherosclerotic lesions in mice. Atherosclerosis 1987;68:231–40.
[15] Ozaki M, Kawashima S, Yamashita T, et al. Overexpression of endothelial nitric oxide synthase accelerates atherosclerotic lesion formation in apoE-deficient mice. J Clin Invest 2002;110:331–40.
[16] Bradford MM. A rapid and sensitive method for the quantification of microgram quantities of protein utilizing the principle of protein-dye binding. Anal Biochem 1972;72:248–54.
[17] Munzel T, Kurz S, Rajagopalan S, et al. Hydralazine prevents nitroglycerin tolerance by inhibiting activation of a membrane-bound NADH oxidase: a new action for an old drug. J Clin Invest 1996;98:1465–70.
[18] Miller FJ, Gutterman DD, Rios CD, Heistad DD, Davidson BL. Superoxide production in vascular smooth muscle contributes to oxidative stress and impaired relaxation in atherosclerosis. Circ Res 1998;82:1298–305.
[19] Alp NJ, Mussa S, Khoo J, et al. Tetrahydrobiopterin-dependent preservation of nitric oxide-mediated endothelial function in diabetes by targeted transgenic GTP-cyclohydrolase I overexpression. J Clin Invest 2003;112:725–35.
[20] Rajagopalan S, Meng XP, Ramasamy S, Harrison DG, Galis ZS. Reactive oxygen species produced by macrophage-derived foam cells regulate the activity of vascular matrix metalloproteinases in vitro. Implications for atherosclerotic plaque stability. J Clin Invest 1996;98:2572–9.
[21] Cai H, Harrison DG. Endothelial dysfunction in cardiovascular diseases: the role of oxidative stress. Circ Res 2000;87:840–4.
[22] Warnholtz A, Nickenig G, Schulz E, et al. Increased NADH-oxidase-mediated superoxide production in the early stages of atherosclerosis: evidence for involvement of the renin-angiotensin system. Circulation 1999;99:2027–33.
[23] Pratico D, Tangirala RK, Rader DJ, Rokach J, FitzGerald GA. Vitamin E suppresses isoprostane generation in vivo and reduces atherosclerosis in ApoE-deficient mice. Nat Med 1998;4:1189–92.
[24] Schwedhelm E, Bartling A, Lenzen H, et al. Urinary 8-*iso*-prostaglandin F2alpha as a risk marker in patients with coronary heart disease: a matched case-control study. Circulation 2004;109:843–8.
[25] Schupp M, Janke J, Clasen R, Unger T, Kintscher U. Angiotensin type 1 receptor blockers induce peroxisome proliferator-activated receptor-gamma activity. Circulation 2004;109:2054–7.
[26] Benson SC, Pershadsingh HA, Ho CI, et al. Identification of telmisartan as a unique angiotensin II receptor antagonist with selective PPAR gamma-modulating activity. Hypertension 2004;43:993–1002.
[27] Sawamura T, Kume N, Aoyama T, et al. An endothelial receptor for oxidized low-density lipoprotein. Nature 1997;386:73–7.

Stoichiometric Relationships Between Endothelial Tetrahydrobiopterin, Endothelial NO Synthase (eNOS) Activity, and eNOS Coupling in Vivo

Insights From Transgenic Mice With Endothelial-Targeted GTP Cyclohydrolase 1 and eNOS Overexpression

Jennifer K. Bendall, Nicholas J. Alp, Nicholas Warrick, Shijie Cai, David Adlam, Kirk Rockett, Mitsuhiro Yokoyama, Seinosuke Kawashima, Keith M. Channon

Abstract—Endothelial dysfunction in vascular disease states is associated with reduced NO bioactivity and increased superoxide ($O_2^{\cdot-}$) production. Some data suggest that an important mechanism underlying endothelial dysfunction is endothelial NO synthase (eNOS) uncoupling, whereby eNOS generates $O_2^{\cdot-}$ rather than NO, possibly because of a mismatch between eNOS protein and its cofactor tetrahydrobiopterin (BH4). However, the mechanistic relationship between BH4 availability and eNOS coupling in vivo remains undefined because no studies have investigated the regulation of eNOS by BH4 in the absence of vascular disease states that cause pathological oxidative stress through multiple mechanisms. We investigated the stoichiometry of BH4–eNOS interactions in vivo by crossing endothelial-targeted eNOS transgenic (eNOS-Tg) mice with mice overexpressing endothelial GTP cyclohydrolase 1 (GCH-Tg), the rate-limiting enzyme in BH4 synthesis. eNOS protein was increased 8-fold in eNOS-Tg and eNOS/GCH-Tg mice compared with wild type. The ratio of eNOS dimer:monomer was significantly reduced in aortas from eNOS-Tg mice compared with wild-type mice but restored to normal in eNOS/GCH-Tg mice. NO synthesis was elevated by 2-fold in GCH-Tg and eNOS-Tg mice but by 4-fold in eNOS/GCH-Tg mice compared with wild type. Aortic BH4 levels were elevated in GCH-Tg and maintained in eNOS/GCH-Tg mice but depleted in eNOS-Tg mice compared with wild type. Aortic and cardiac $O_2^{\cdot-}$ production was significantly increased in eNOS-Tg mice compared with wild type but was normalized after NOS inhibition with *N*ω-nitro-L-arginine methyl ester hydrochloride (L-NAME), suggesting $O_2^{\cdot-}$ production by uncoupled eNOS. In contrast, in eNOS/GCH-Tg mice, $O_2^{\cdot-}$ production was similar to wild type, and L-NAME had no effect, indicating preserved eNOS coupling. These data indicate that eNOS coupling is directly related to eNOS–BH4 stoichiometry even in the absence of a vascular disease state. Endothelial BH4 availability is a pivotal regulator of eNOS activity and enzymatic coupling in vivo. (***Circ Res.* 2005;97:864-871.**)

Key Words: endothelial nitric oxide synthase ■ tetrahydrobiopterin ■ nitric oxide ■ superoxide

Nitric oxide (NO), produced by endothelial NO synthase (eNOS) in the vascular endothelium, is a critical signaling molecule in vascular homeostasis.[1] NO serves as an endothelium-derived relaxing factor, regulates vasomotor tone and blood pressure,[1,2] and has multiple antiatherogenic roles by inhibiting vascular smooth muscle cell proliferation, platelet aggregation, and leukocyte adhesion.[1] Loss of NO bioavailability is a key feature of endothelial dysfunction in vascular disease states such as hypertension, diabetes, and atherosclerosis. Furthermore, impaired NO-mediated endothelial function is an independent risk factor for cardiovascular disease.[3–5] Several factors contribute to loss of NO bioavailability, including reduced NO synthesis and NO scavenging by reactive oxygen species (ROS).[6] Under physiological conditions, there is a balance between endothelial NO and ROS production. However, vascular diseases are associated with increased ROS generation.[6] Several oxidase systems contribute to the increased oxidative stress, notably the NADPH oxidases.[7,8]

Increasing evidence suggests that eNOS itself can generate superoxide ($O_2^{\cdot-}$) under certain pathophysiological conditions.[9] Ozaki et al[10] reported recently that transgenic overexpression of eNOS in apolipoprotein E knockout mice paradoxically increases vascular $O_2^{\cdot-}$ production because of

Original received March 9, 2005; revision received August 10, 2004; accepted September 12, 2005.

From the Department of Cardiovascular Medicine (J.K.B., N.J.A., N.W., S.C., D.A., K.M.C.), University of Oxford, John Radcliffe Hospital, United Kingdom; Childhood Infection Group (K.R.), Wellcome Trust Centre for Human Genetics, University of Oxford, United Kingdom; and Kobe University School of Medicine (M.Y., S.K.), Japan.

Correspondence to Professor Keith M. Channon, Department of Cardiovascular Medicine, John Radcliffe Hospital, Oxford, OX3 9DU, UK. E-mail keith.channon@cardiov.ox.ac.uk

Circulation Research is available at http://circres.ahajournals.org

DOI: 10.1161/01.RES.0000187447.03525.72

enzymatic uncoupling of increased eNOS protein levels. Recent data indicate that the pterin cofactor tetrahydrobiopterin (BH4) is a major determinant of whether eNOS produces NO or $O_2^{\cdot-}$.[11,12] When BH4 levels are insufficient, there is a shift toward the production of $O_2^{\cdot-}$ as electron transfer within the active site of eNOS becomes uncoupled from L-arginine oxidation, and molecular oxygen is instead reduced to form $O_2^{\cdot-}$.[11] $O_2^{\cdot-}$ generated by eNOS has been implicated in endothelial dysfunction associated with a number of vascular disease states, including diabetes, smoking, hypertension, and atherosclerosis,[10,12–16] and BH4 supplementation improves endothelium-dependent vasodilatation under these conditions.[16] However, the effects of systemic pharmacological BH4 supplementation in these studies may be mediated in part by nonspecific antioxidant properties of acute high-dose BH4,[17] which can increase NO bioavailability indirectly by reducing its scavenging by ROS.

Recent studies have focused on the potential role of BH4 oxidation, to dihydrobiopterin (BH2) and other biopterin species, in reducing BH4 bioavailability in preatherosclerotic disease states.[16–18] In particular, the interaction of BH4 with peroxynitrite (generated from the reaction between NO and $O_2^{\cdot-}$) rapidly oxidizes BH4 and can provoke eNOS uncoupling and endothelial dysfunction.[12,19–21] Indeed, eNOS uncoupling may exacerbate the process by contributing to BH4 oxidation. However, it is unclear whether eNOS uncoupling alone is sufficient to initiate BH4 oxidation and exacerbate eNOS uncoupling in vivo because all in vivo studies to date have evaluated BH4-dependent eNOS regulation in complex vascular disease states in which multiple inflammatory and redox pathways are implicated. Other previous studies of the role of BH4 in eNOS function have relied on purified recombinant proteins in reconstituted cell-free systems.[9,11,22,23]

Accordingly, we sought to investigate the importance of BH4 in regulating eNOS activity in vivo in healthy animals without vascular disease. We used a transgenic mouse model with endothelial-targeted overexpression of GTP cyclohydrolase 1 (GTPCH), the rate-limiting enzyme in BH4 synthesis, in which endothelial BH4 levels are specifically increased.[24] We crossed this transgenic mouse with a mouse overexpressing eNOS in the endothelium to generate mouse models with graded alterations in endothelial BH4 and eNOS levels to investigate the mechanistic relationships between BH4 and eNOS coupling in vivo.

Materials and Methods

Animals

All studies involving laboratory animals were conducted in accordance with the UK Home Office Animals (Scientific Procedures) Act 1986 (HMSO, UK). eNOS transgenic (eNOS-Tg) mice, in which bovine eNOS transgene overexpression is targeted to the vascular endothelium under the control of the murine preproendothelin-1 promoter in a C57BL/6 background, were produced as described previously.[25] GTPCH transgenic (GCH-Tg) mice, in which human GTPCH transgene overexpression is targeted to the endothelium under control of the murine Tie-2 promoter, were generated in a C57BL/6 background as described previously.[26] Heterozygote eNOS-Tg mice were mated with heterozygote GCH-Tg mice to produce experimental eNOS/GCH-Tg, eNOS-Tg, GCH-Tg, and wild-type littermates in a 1:1:1:1 ratio. Mice (between 13 and 20 weeks of age in all experiments) were housed in individually ventilated cages with 12-hour light/dark cycle and controlled temperature (20°C to 22°C) and fed normal chow and water ad libitum.

Western Blot Analysis

Lung samples ($n \geq 4$ per group) were homogenized on ice for 20 seconds in lysis buffer (50 mmol/L Tris, pH 7.5, 150 mmol/L NaCl, 0.1% SDS, 0.5% deoxycholate, 1% Nonidet P-40) containing protease inhibitors (Complete; Boehringer Mannheim) and 1 mmol/L phenylmethylsulfonyl fluoride. Protein lysates (8 μg) were resolved using SDS-PAGE and transferred to polyvinylidene difluoride membranes. Membranes were incubated with a 1:2000 dilution of mouse anti-eNOS monoclonal antibody (Transduction Laboratories), which recognizes murine and bovine eNOS, followed by a 1:2500 dilution of rabbit anti-mouse horseradish peroxidase–conjugated secondary antibody (Promega). Protein bands were visualized by chemiluminescence. To investigate the ratio of eNOS homodimer to monomer, Western blots were performed as above using nonboiled aortic lysates and low-temperature SDS-PAGE as described previously.[27]

Primary Cultures of Murine Lung Endothelial Cells

Lungs were harvested into culture medium (35% DMEM, 35% Ham's F-10 nutrient mixture, 20% FBS, 2 mmol/L L-glutamine, 100 U/100 μg/mL penicillin–streptomycin, 100 μg/mL heparin, and 50 μg/mL endothelial mitogen [Biogenesis]), cut into 1- to 2-mm pieces and digested using 0.1% collagenase type I for 1 hour at 37°C. The lung digest was passed through a 100-μm cell strainer. Cells were centrifuged, resuspended in culture medium, and plated onto 0.1% gelatin-coated cover slips. Cultures were maintained at 37°C in humidified 5% CO_2/95% air atmosphere for 72 hours before fixation with 4% paraformaldehyde.

Immunocytochemistry

Fixed cultures were permeabilized with PBS containing 0.5% Triton X-100, and nonspecific staining was reduced by blocking with 10% normal goat serum. Cultures were incubated with a polyclonal rabbit anti-eNOS primary antibody (Transduction Laboratories) followed by goat anti-rabbit secondary antibody (Alexa Fluor 488; Molecular Probes). Cells were mounted with cover slips using Vectashield containing propidium iodide (Vector Laboratories) and imaged using a Bio-Rad MRC-1024 laser-scanning confocal microscope.

Measurement of Biopterins and Neopterin

Biopterins, such as BH4, BH2 and biopterin, and neopterin were measured in aortic homogenates by high-performance liquid chromatography (HPLC) analysis after iodine oxidation in acidic or alkaline conditions as described previously.[24,28] In brief, thoracic aortas ($n=6$ to 8 per group) were homogenized for 20 seconds in ice-cold extract buffer (50 mmol/L Tris-HCl, pH 7.4, 1 mmol/L dithiothreitol, and 1 mmol/L EDTA) containing 0.1 μmol/L neopterin as an internal recovery standard. Samples were deproteinated before undergoing oxidation with 1% iodine/2% potassium iodide under either acidic or basic conditions. Biopterin content was assessed using HPLC in 5% methanol/95% water using an ACE 5 C18 column (ACT) and fluorescence detection (350 nm excitation and 450 nm emission). BH4 concentration was calculated as picomoles per milligram of protein by subtracting BH2 and biopterin from total biopterin content.

Arginine-to-Citrulline Conversion

NOS enzymatic activity, and indirectly NO synthesis, was measured by the conversion of ^{14}C L-arginine to ^{14}C L-citrulline in fresh intact aorta ($n=5$ to 8 per group) and lung homogenate ($n=6$ per group) as described previously.[24,29] The integrals of citrulline peaks were expressed as a proportion of total ^{14}C counts for each sample.

Electron Paramagnetic Resonance Spectroscopy

Electron paramagnetic resonance (EPR) spectroscopy was used to quantify vascular NO production according to previously described and validated methods.[30] In brief, freshly harvested aortas (n=8 to 11 per group) were stimulated with calcium ionophore (A23187; 1 μmol/L) in 100 μL Krebs–HEPES buffer, then incubated with colloid iron (II) diethyldithiocarbamate [Fe(DETC)$_2$] (285 μmol/L) at 37°C for 90 minutes. After incubation, aortas were snap-frozen in a column of Krebs–HEPES buffer in liquid nitrogen, and EPR spectra were obtained using an X-band EPR spectrometer (Miniscope MS 200; Magnettech). Signals were quantified by measuring the total amplitude, after correction of baseline, and after subtracting background signals from incubation with colloid Fe(DETC)$_2$ alone.

Lucigenin-Enhanced Chemiluminescence Detection of Superoxide in Heart Lysates

Basal $O_2^{\cdot-}$ production was measured in left ventricular (LV) homogenates (n=7 to 10 per group) using the technique of lucigenin (5 μmol/L) chemiluminescence according to methods described previously.[14,31] In brief, hearts were flushed with ice-cold Krebs–HEPES buffer, the LV excised, and snap-frozen in liquid nitrogen. Samples were homogenized in Kreb–HEPES buffer containing protease inhibitors (Complete; Boehringer Mannheim) at pH 7.4. Chemiluminescence was measured in a FB12 luminometer (Berthold Detection Systems) at 37°C. Chemiluminescence of 200 μg LV protein was recorded every minute for 8 minutes. The NOS inhibitor *N*ω-nitro-L-arginine methyl ester hydrochloride (L-NAME; 1 mmol/L) was subsequently added and chemiluminescence recorded for an additional 5 minutes. Background readings were subtracted from sample readings and results expressed as counts per second.

Lucigenin-Enhanced Chemiluminescence Detection of Superoxide in Intact Aorta

Basal $O_2^{\cdot-}$ production was measured in intact aorta (n=8 to 12 per group) according to methods described previously.[14,32] In brief, freshly cleaned and harvested thoracic aortas were opened longitudinally, cut into 2, and transferred to ice-cold Krebs–HEPES buffer. Vessels were equilibrated in Krebs–HEPES buffer gassed with 95% oxygen/5% carbon dioxide for 30 minutes at 37°C, with one half of each vessel being incubated in the presence of L-NAME (1 mmol/L). Lucigenin (20 μmol/L) chemiluminescence was then recorded every minute for 10 minutes as above. Background readings were subtracted from sample readings and results expressed as counts per second per milligram dry weight of aorta.

Oxidative Fluorescent Microtopography

$O_2^{\cdot-}$ production in tissue sections of mouse aorta (n=5 to 7 per group) was detected using the fluorescent probe dihydroethidium (DHE), as described previously.[14,24,33] Fresh segments of thoracic aorta were frozen in optimal cutting temperature compound. Cryosections (30 μm) were incubated with Krebs–HEPES buffer with or without L-NAME (1 mmol/L; to inhibit eNOS) for 30 minutes at 37°C, then for an additional 5 minutes with DHE (2 μmol/L; Molecular Probes). Images were obtained using a Bio-Rad laser-scanning confocal microscope, equipped with a krypton/argon laser, using identical acquisition settings for each section. DHE fluorescence was quantified by automated image analysis using Image-Pro Plus software (Media Cybernetics). DHE fluorescence from high power (×60) images was measured only on the luminal side of the internal elastic lamina to quantify endothelial cell fluorescence. For each vessel, mean fluorescence was calculated from 4 separate high-power fields taken in each quadrant of the vessel to produce n=1, and all experiments were performed in a batch design.

Statistical Analysis

One-way ANOVA tests were used to compare data sets, with appropriate post hoc correction for multiple comparisons. $P<0.05$ was considered significant. Data are expressed as means and SEM.

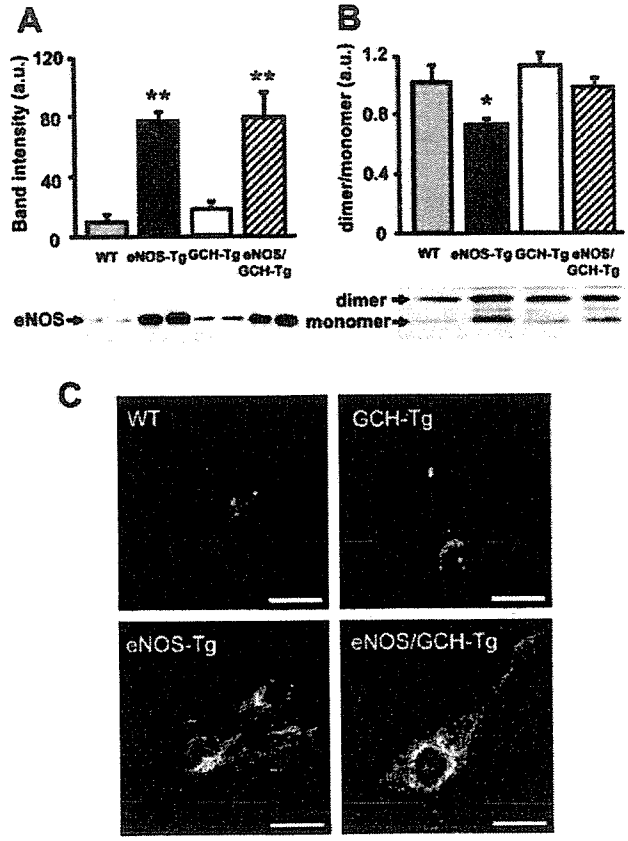

Figure 1. Immunoblotting with a murine anti-eNOS monoclonal antibody to detect native and transgenic eNOS monomer protein in boiled lung lysates (A) and eNOS dimer:monomer protein bands in aortic lysates from wild-type (WT), eNOS-Tg, GCH-Tg, and eNOS/GCH-Tg mice (B); n=4 animals per group; *$P<0.05$ and **$P<0.001$ compared with WT. a.u. indicates arbitrary units. C, Immunofluorescent detection of eNOS (green), counterstained with propidium iodide (red), in primary endothelial cells cultured from WT, eNOS-Tg, GCH-Tg, and eNOS/GCH-Tg mice. Bar=20 μm.

Results

eNOS Protein Levels and Subcellular Localization

Western blot analysis confirmed that eNOS protein levels were elevated 8-fold in eNOS-Tg compared with wild-type animals ($P<0.001$; Figure 1A). Overexpression of endothelial GTPCH, the rate-limiting enzyme in BH4 synthesis, in GCH-Tg mice did not significantly alter eNOS protein levels compared with wild type. However, as for eNOS-Tg mice, eNOS protein levels were elevated 8-fold in double-transgenic eNOS/GCH-Tg mice.

We used low-temperature SDS-PAGE and immunoblotting to investigate eNOS homodimerization and the ratio of eNOS dimer to monomer in aortas. In eNOS-Tg aortas, eNOS dimer:monomer was significantly depleted compared with wild type ($P<0.05$) but unchanged in GCH-Tg mice (Figure 1B). Importantly, the reduced eNOS dimer:monomer ratio in the eNOS-Tg group was restored to wild-type levels in double- transgenic eNOS/GCH-Tg mice.

We investigated the subcellular localization of eNOS in primary cultures of lung endothelial cells using immunocytochemistry. eNOS appeared to be localized mainly to plasma

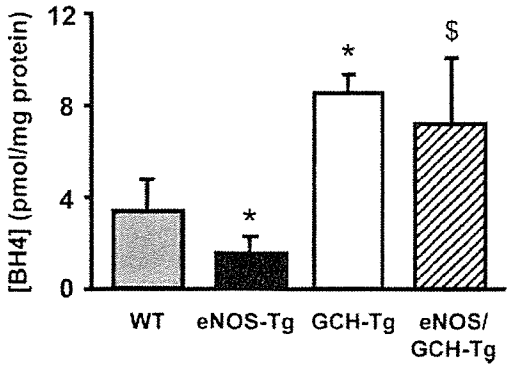

Figure 2. BH4 levels in aortas from wild-type (WT), eNOS-Tg, GCH-Tg, and eNOS/GCH-Tg mice. *$P<0.05$ compared with WT and \$$P<0.05$ compared with eNOS-Tg; n=6 to 8 animals per group.

membranes and the Golgi apparatus in endothelial cells from all 4 groups (Figure 1C). However, in accordance with the immunoblotting data, the intensity of eNOS immunostaining, unchanged in GCH-Tg mice, was markedly increased in endothelial cells from eNOS-Tg and eNOS/GCH-Tg animals compared with wild type.

Aortic BH4 Levels

We next measured vascular BH4 levels in homogenates of snap-frozen aorta using iodine oxidation and HPLC. Surprisingly, BH4 levels were significantly depleted in eNOS-Tg mice compared with wild type, suggesting oxidative degradation of BH4 ($P<0.05$; Figure 2). We then sought to confirm that increased endothelial GTPCH expression led to increased BH4 levels in aortic homogenates of GCH-Tg and eNOS/GCH-Tg mice. As reported previously,[24] aortic BH4 levels were significantly elevated by >2-fold in GCH-Tg mice compared with wild type ($P<0.05$). Importantly, aortic BH4 levels were also elevated in eNOS/GCH-Tg mice and were not significantly different between GCH-Tg and eNOS/GCH-Tg mice.

eNOS Enzymatic Activity and NO Production

To determine the relationship between eNOS protein levels and eNOS enzymatic activity, we measured conversion of ^{14}C L-arginine to ^{14}C L-citrulline by eNOS in intact aorta using HPLC with online scintillation detection. Citrulline production was increased only 2-fold in eNOS-Tg aortas compared with wild type ($P<0.05$; Figure 3A and 3B), despite eNOS protein levels being elevated 8-fold in these animals. Indeed, the ratio of eNOS enzymatic activity to eNOS protein was 0.6 in eNOS-Tg mice compared with 2.0 in wild-type animals. A similar pattern of results was obtained when using lung tissue lysates (Figure 3C). To further investigate the stoichiometric relationship between eNOS and endothelial BH4 in vivo and to determine whether increasing endothelial BH4 in eNOS-Tg mice could augment eNOS enzymatic activity, we next measured eNOS enzymatic activity in GCH-Tg and eNOS/GCH-Tg mice. NOS activity was increased 2-fold in GCH-Tg aorta and lung compared with wild type ($P<0.05$; Figure 3A through 3C). Indeed, eNOS enzymatic activity was similar in GCH-Tg and eNOS-Tg mice despite eNOS protein

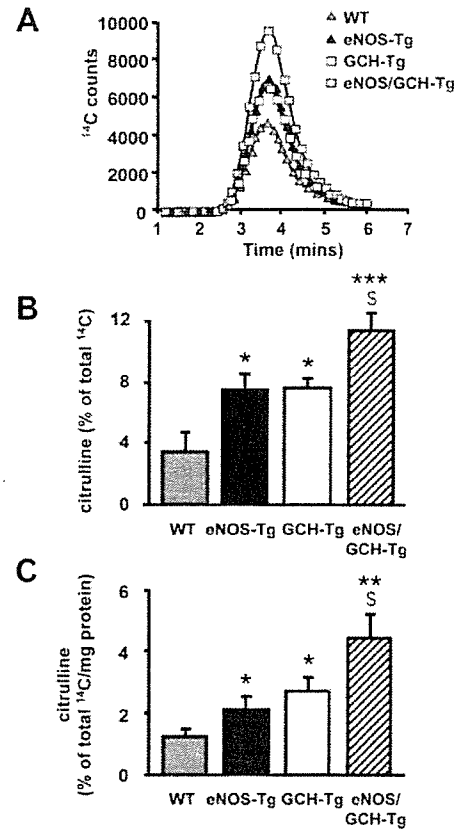

Figure 3. A, Representative HPLC chromatograms showing ^{14}C citrulline peaks for wild-type (WT; gray triangles), eNOS-Tg (black triangles), GCH-Tg (white squares), and eNOS/GCH-Tg (hatched squares) mouse aortas. Graphs show percentage ^{14}C citrulline conversion from ^{14}C arginine as a measure of eNOS activity measured in total fresh intact aorta (B) and lung tissue lysates (C); n=5 to 8 animals per group; *$P<0.05$, **$P<0.01$, and ***$P<0.001$ compared with WT; and \$$P<0.05$ compared with eNOS-Tg.

levels being considerably higher in eNOS-Tg animals. Critically, eNOS enzymatic activity was further elevated in eNOS/GCH-Tg mice compared with eNOS-Tg animals ($P<0.05$): augmented levels of endothelial BH4 in eNOS/GCH-Tg mice resulted in an ≈4-fold increase in eNOS enzymatic activity in aorta and lung compared with wild-type mice ($P<0.01$). These data suggest that eNOS activity is exquisitely dependent on endothelial BH4 levels even in the absence of vascular disease.

In complementary experiments, we used Fe-DETC EPR to directly measure NO bioavailability in mouse aortas. In accordance with measures of enzymatic activity, net NO levels were increased ≈2-fold in eNOS-Tg aortas compared with wild type (Figure 4). These results demonstrate that there was a striking discordance between eNOS protein levels, eNOS enzymatic activity, and NO production in eNOS-Tg mice. We then determined the effects of increased endothelial BH4 using the GCH-Tg and eNOS/GCH-Tg mice and observed a similar pattern of results as for NOS enzymatic activity. Aortic NO bioavailability was elevated almost 2-fold in GCH-Tg mice compared with wild type and not significantly different from eNOS-Tg mice (Figure 4). Criti-

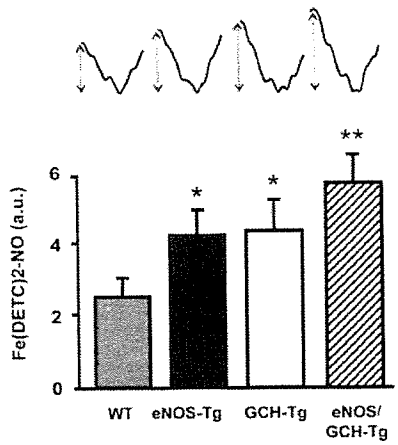

Figure 4. Net NO levels in intact aorta measured using Fe-DETC EPR. Graph shows mean quantitative data with corresponding representative EPR spectra showing the characteristic peaks associated with the Fe-DETC signal above. n=8 to 11 animals per group; *$P<0.05$ and **$P<0.01$ compared with wild type (WT). a.u. indicates arbitrary units.

cally, net NO bioavailability was further elevated (≈3-fold compared with wild type) in eNOS/GCH-Tg mice.

eNOS Uncoupling: Effect of eNOS and GTPCH Overexpression In Vivo

To investigate whether eNOS uncoupling results from discordance between eNOS and BH4, we measured $O_2^{\cdot-}$ production and, more specifically, eNOS-derived $O_2^{\cdot-}$ production using the NOS inhibitor L-NAME. We first measured $O_2^{\cdot-}$ production in tissue lysates using lucigenin chemiluminescence. Chemiluminescence was increased 2-fold in eNOS-Tg mice compared with wild-type animals ($P<0.05$; Figure 5A) but was unchanged in GCH-Tg mice. Critically, $O_2^{\cdot-}$ production was restored in eNOS/GCH-Tg mice. The proportion of $O_2^{\cdot-}$ production attributable to uncoupled NOS, assessed by quantifying L-NAME–inhibitable chemiluminescence, was significantly increased in eNOS-Tg lysates compared with wild type, indicating increased NOS uncoupling ($P<0.05$; Figure 5B). L-NAME–inhibitable chemiluminescence was unchanged in GCH-Tg mice. The presence of the GTPCH transgene in eNOS/GCH-Tg mice restored the enhanced L-NAME–inhibitable chemiluminescence of the eNOS-Tg group back to wild-type levels. We also investigated $O_2^{\cdot-}$ production in intact aorta under basal conditions and after incubation with L-NAME using lucigenin chemiluminescence and saw a similar pattern of results. Basal chemiluminescence was significantly increased in eNOS-Tg aortas compared with wild type ($P<0.05$; Table). Importantly, basal $O_2^{\cdot-}$ production in GCH-Tg and eNOS/GCH-Tg aortas was similar to wild type. Incubation of aortas with L-NAME caused a significant reduction in the $O_2^{\cdot-}$ signal in eNOS-Tg mice ($P<0.05$), indicating NOS uncoupling. However, L-NAME had little effect in wild-type, GCH-Tg, and eNOS/GCH-Tg aortas, suggesting that NOS coupling is preserved in these mice. Together, these observations suggest that in eNOS-Tg mice elevated $O_2^{\cdot-}$ production is at least partly attributable to uncoupled NOS, likely resulting from discordance between eNOS protein and endothelial BH4 because NOS coupling is preserved by increasing endothelial BH4 in association with elevated eNOS levels in eNOS/GCH-Tg animals.

Lucigenin Chemiluminescence to Measure $O_2^{\cdot-}$ Production in Intact Aortas Incubated for 30 Minutes at 37°C in the Presence or Absence of L-NAME (1 mmol/L)

	Wild Type	eNOS-Tg	GCH-Tg	eNOS/GCH-Tg
Basal, RLU/s/mg	39.5±4.5	59.7±6.6*	52.8±5.8	46.2±4.7
+ L-NAME, RLU/s/mg	42.5±10.1	39.2±4.8†	54.0±13.2	49.3±11.2

Results are expressed as counts per second per milligram of dry weight of aorta.

*$P<0.05$compared with wild type; †$P<0.05$ compared with baseline (without L-NAME).

RLU indicates relative light units.

To investigate $O_2^{\cdot-}$ production specifically from the aortic endothelium, we quantified endothelial DHE fluorescence using oxidative confocal microtopography. Endothelial DHE fluorescence was increased 2-fold in eNOS-Tg mice compared with wild-type and GCH-Tg mice (Figure 6). Impor-

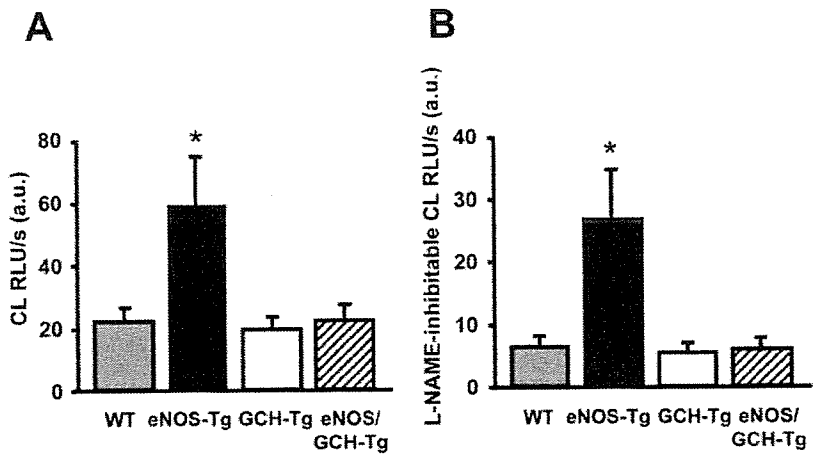

Figure 5. Lucigenin (5μmol/L) chemiluminescence (CL) in cardiac tissue lysates from wild-type (WT), eNOS-Tg, GCH-Tg, and eNOS/GCH-Tg mice to measure basal $O_2^{\cdot-}$ production (A) and L-NAME (1 mmol/L)–inhibitable $O_2^{\cdot-}$ production (B) as a marker of NOS uncoupling. *$P<0.05$ compared with WT; n=7 to 10 animals per group. RLU indicates relative light units; a.u., arbitrary units.

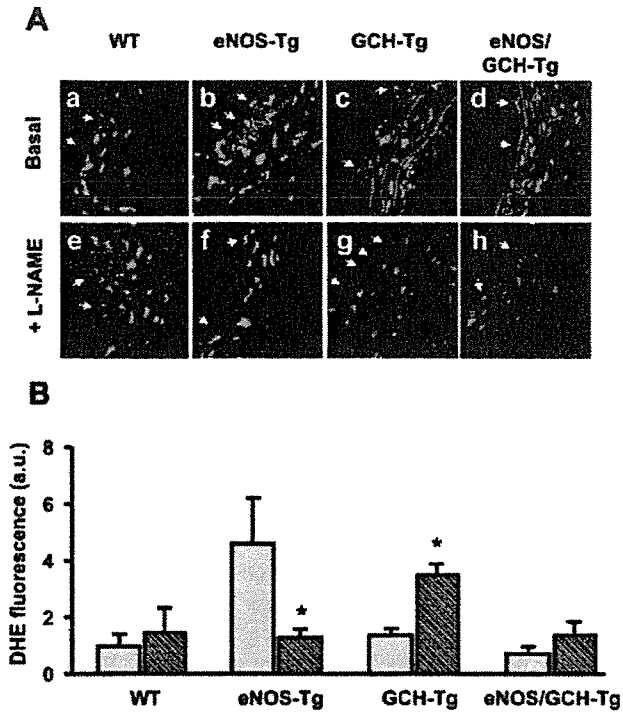

Figure 6. DHE staining, to measure in situ $O_2^{\cdot-}$ production, in aortic sections. A, Representative aortic sections (×60) showing red endothelial cells (arrows) from wild-type (WT; a and e), eNOS-Tg (b and f), GCH-Tg (c and g), and eNOS/GCH-Tg (d and h) mice in the presence (e through h) and absence (a through d) of L-NAME (1 mmol/L). B, Quantified specific endothelial DHE fluorescence is expressed for sections in the presence (hatched bars) and absence (gray bars) of L-NAME in arbitrary units (a.u.) for each group. *$P<0.05$ comparing sections in the presence or absence of L-NAME; n=5 to 7 animals per group.

tantly, endothelial fluorescence was restored to wild-type levels in eNOS/GCH-Tg mice. Fluorescence from the other layers of the vessel wall was not significantly different between groups. Incubation with L-NAME had little effect in wild-type aortas but reversed the elevated DHE signal in eNOS-Tg endothelium back to wild-type levels, again indicating that the source of $O_2^{\cdot-}$ was likely uncoupled eNOS. In contrast, L-NAME significantly increased the endothelial $O_2^{\cdot-}$ signal in GCH-Tg mice, indicating that in these aortas, eNOS was predominantly coupled and producing NO. Critically, as in wild-type aortas, NOS inhibition with L-NAME had little effect in eNOS/GCH-Tg mice, indicating restored eNOS coupling compared with eNOS-Tg animals. In accordance with the data for $O_2^{\cdot-}$ production measured by chemiluminescence, these results suggest that increased eNOS uncoupling in eNOS-Tg aortas increases eNOS-derived $O_2^{\cdot-}$, but that eNOS coupling is, at least in part, preserved by increased endothelial BH4 synthesis in eNOS/GCH-Tg mice.

Discussion

In this study, we describe a new double-transgenic mouse model in which endothelial-targeted overexpression of GTPCH leads to increased endothelial BH4 levels in mice with endothelial-targeted eNOS overexpression. We used this model to investigate the role of BH4 in the regulation of eNOS coupling in vivo, specifically in the absence of pathological oxidative stress associated with vascular disease states.[6] The major findings in this study are as follows. First, eNOS protein levels are markedly elevated in eNOS-Tg and eNOS/GCH-Tg mice but not in GCH-Tg animals, although the proportion of eNOS dimer to monomer is depleted only in eNOS-Tg aortas. Second, endothelial-specific overexpression of GTPCH is sufficient to increase vascular BH4 levels in GCH-Tg and in eNOS/GCH-Tg aortas, whereas BH4 levels are depleted in eNOS-Tg aortas. Third, this increase in BH4 is sufficient to augment vascular eNOS enzymatic activity even in GCH-Tg mice, which have unchanged eNOS protein levels. Indeed, eNOS activity is similar between GCH-Tg and eNOS-Tg mice despite eNOS-Tg mice having 8-fold more eNOS protein. Importantly, the increase in endothelial BH4 in eNOS/GCH-Tg mice further enhances eNOS activity and NO bioavailability compared with eNOS-Tg mice. Fourth, the discordance between endothelial BH4 and eNOS protein in eNOS-Tg mice results in uncoupled eNOS and increased NOS-derived $O_2^{\cdot-}$ production in tissue lysates and intact aorta. However, increased vascular BH4 in eNOS/GCH-Tg mice is sufficient, at least in part, to restore eNOS coupling, increase NO production, and reduce eNOS-dependent $O_2^{\cdot-}$ production.

These findings provide important insights into the role of endothelial BH4 synthesis in regulating eNOS activity and eNOS coupling even in the absence of vascular oxidative stress. Previous studies have reported that endothelial dysfunction in vascular diseases, such as hypertension,[12] diabetes,[24] and atherosclerosis,[26] is associated with increased $O_2^{\cdot-}$ production deriving principally from NADPH oxidases.[7,8] Landmesser et al[12] demonstrated that the increase in NADPH oxidase–derived $O_2^{\cdot-}$ in deoxycorticosterone acetate–salt hypertensive mice led to enhanced oxidation of BH4, resulting in eNOS uncoupling, increased eNOS-derived $O_2^{\cdot-}$ production, and reduced NO formation, thereby exacerbating oxidative stress. Oral supplementation with BH4, or a reduction in NADPH oxidase activity (using p47phox−/− mice), reversed eNOS uncoupling. However, the mechanistic relationship between eNOS and its cofactor BH4 has not been investigated in vivo in the absence of pathological oxidative stress. We now show that a stoichiometric discordance between eNOS protein and BH4 levels is alone sufficient to cause eNOS uncoupling, and that eNOS uncoupling in the absence of vascular disease is sufficient to deplete BH4 levels by oxidation. Laursen et al[19] demonstrated that peroxynitrite may be the principal ROS involved in oxidation of BH4.

NO, constitutively produced by eNOS in the vascular endothelium, is a potent vasodilator and exerts numerous vasoprotective antiatherogenic effects. Reduced NO bioactivity is an early feature of a number of vascular diseases, including atherosclerosis.[5] Short-term in vivo gene transfer of eNOS or neuronal NOS can improve NO-mediated vascular relaxation in atherosclerotic arteries.[34] However, previous studies investigating the possible vasoprotective effects of chronic eNOS overexpression in eNOS-Tg mice have yielded conflicting results. Kawashima et al[35] demonstrated reduced lesion formation after carotid artery ligation in eNOS-Tg mice. In contrast, Ozaki et al,[10] using the same strain of

eNOS-Tg mice as used in the present study, found that eNOS overexpression accelerated rather than reduced atherosclerosis in apolipoprotein E knockout mice, at least in part, because of eNOS uncoupling and $O_2^{\cdot-}$ generation. In the present study, using a mouse model not exposed to pathological vascular oxidative stress, we also show that eNOS-derived $O_2^{\cdot-}$ production is enhanced in eNOS-Tg mice, in cardiac tissue lysates and intact aorta, indicating increased eNOS uncoupling in these animals. We performed additional experiments, using quantitative RT-PCR, to confirm that the increased $O_2^{\cdot-}$ in eNOS-Tg animals is not a result of a concomitant increase in the expression of the NADPH oxidase system, a major source of vascular $O_2^{\cdot-}$ generation (data not shown). These findings agree with those from Ohashi et al[25] using nondiseased eNOS-Tg mice. This enhanced vascular oxidative stress may account for the depleted aortic BH4 levels observed in the eNOS-Tg mice because BH4 is readily oxidized by ROS to BH2 that is inactive for eNOS cofactor function. In accordance with having increased uncoupled eNOS and depleted BH4 levels, specific NOS enzymatic activity is markedly attenuated in eNOS-Tg mice (elevated only 2-fold compared with wild type) relative to eNOS protein levels (elevated 8-fold compared with wild type). Indeed, the ratio of eNOS enzymatic activity to eNOS protein was only 0.6 in eNOS-Tg mice compared with 2.0 in wild-type animals.

Several previous studies have established that BH4 is a required cofactor for NOS activity.[9,28,36] Recent studies, including those in atherosclerotic eNOS-Tg mice,[10] have demonstrated that NOS uncoupling can be reversed and NOS enzymatic activity increased by augmenting BH4 levels.[10,12] However, an advantage of the present study is that by targeting overexpression of GTPCH, the rate-limiting enzyme in BH4 biosynthesis, to the vascular endothelium, we avoid the potential confounding antioxidant effects of high-dose pharmacological BH4 supplementation used in other studies.[10,12] Furthermore, we have been able to specifically evaluate the role of endothelial BH4, as opposed to systemic BH4, in the regulation of eNOS activity. Importantly, using 2 methods to measure $O_2^{\cdot-}$ production in cardiac tissue and intact aorta, as well as specifically in aortic endothelium, we demonstrate that NOS-dependent $O_2^{\cdot-}$ generation, elevated in eNOS-Tg mice, is normalized in eNOS/GCH-Tg mice. These data support the hypothesis that discordance between eNOS protein and endothelial BH4 levels is sufficient to cause eNOS uncoupling even in the absence of pathological oxidative stress. In support of this conclusion, NOS enzymatic activity and the ratio of enzymatic activity relative to eNOS protein levels were increased in eNOS/GCH-Tg compared with eNOS-Tg mice. Interestingly, GCH-Tg mice also had increased NOS enzymatic activity compared with wild type, indicating that even in the absence of either enhanced eNOS protein or disease, BH4 levels may limit eNOS enzymatic activity in vivo. These data therefore suggest that eNOS activity (to generate NO) can be augmented by modestly increasing BH4 levels, specifically in the endothelium, even under normal physiological conditions.

Previous data have shown that eNOS dimerization is an important aspect of eNOS activation and NO production.[28] BH4 has been suggested to increase the stability of the eNOS homodimer such that the ratio of dimer to monomer is increased.[28,37] In eNOS-Tg mice, the discordance between high levels of eNOS protein and depleted aortic BH4 levels may account for the relative decrease in homodimeric eNOS protein that we observed. In support, the increased production of endothelial BH4 in eNOS/GCH-Tg mice was sufficient to maintain the ratio of eNOS dimer to monomer. These in vivo findings corroborate previous in vitro studies suggesting that an important action of BH4, in addition to its direct contribution to electron transport within the eNOS active site, is to maintain eNOS in its homodimeric conformation.

We conclude that eNOS uncoupling is an independent and direct consequence of a stoichiometric discordance between enzyme and its cofactor BH4. BH4 is critical for regulating eNOS activity and its production of NO, as opposed to $O_2^{\cdot-}$, even in the absence of increased oxidative stress associated with vascular disease states. Thus, strategies to increase eNOS protein without a concomitant augmentation of endothelial BH4 levels may lead to eNOS uncoupling and paradoxically exacerbate oxidative stress and the progression of vascular diseases. Although reduced biosynthesis of BH4 may not be the principal mechanism of BH4 loss in vascular disease, strategies aimed at increasing BH4 synthesis or reducing BH4 oxidation may be valid therapeutic approaches in vascular disease states.

Acknowledgments

This work was supported by the British Heart Foundation (RG02/007) and the Wellcome Trust.

References

1. Ignarro LJ. Nitric oxide as a unique signaling molecule in the vascular system: a historical overview. *J Physiol Pharmacol.* 2002;53:503–514.
2. Furchgott RF, Zawadzki JV. The obligatory role of endothelial cells in the relaxation of arterial smooth muscle by acetylcholine. *Nature.* 1980;288:373–376.
3. Panza JA, García CE, Kilcoyne CM, Quyyumi AA, Cannon RO III. Impaired endothelium-dependent vasodilation in patients with essential hypertension: evidence that nitric oxide abnormality is not localized to a single signal transduction pathway. *Circulation.* 1995;91:1732–1738.
4. Schachinger V, Britten MB, Zeiher AM. Prognostic impact of coronary vasodilator dysfunction on adverse long-term outcome of coronary heart disease. *Circulation.* 2000;101:1899–1906.
5. Heitzer T, Schlinzig T, Krohn K, Meinertz T, Munzel T. Endothelial dysfunction, oxidative stress, and risk of cardiovascular events in patients with coronary artery disease. *Circulation.* 2001;104:2673–2678.
6. Cai H, Harrison DG. Endothelial dysfunction in cardiovascular diseases: the role of oxidant stress. *Circ Res.* 2000;87:840–844.
7. Griendling KK, Sorescu D, Ushio-Fukai M. NAD(P)H oxidase: role in cardiovascular biology and disease. *Circ Res.* 2000;86:494–501.
8. Guzik TJ, West NEJ, Black E, McDonald D, Ratnatunga C, Pillai R, Channon KM. Vascular superoxide production by NAD(P)H oxidase: association with endothelial dysfunction and clinical risk factors. *Circ Res.* 2000;86:e85–e90.
9. Vasquez-Vivar J, Kalyanaraman B, Martasek P, Hogg N, Masters BS, Karoui H, Tordo P, Pritchard KA Jr. Superoxide generation by endothelial nitric oxide synthase: the influence of cofactors. *Proc Natl Acad Sci U S A.* 1998;95:9220–9225.
10. Ozaki M, Kawashima S, Yamashita T, Hirase T, Namiki M, Inoue N, Hirata K-i, Yasui H, Sakurai H, Yoshida Y, Masada M, Yokoyama M. Overexpression of endothelial nitric oxide synthase accelerates atherosclerotic lesion formation in apoE-deficient mice. *J Clin Invest.* 2002;110:331–340.
11. Vasquez-Vivar J, Kalyanaraman B, Martasek P. The role of tetrahydrobiopterin in superoxide generation from eNOS: enzymology and physiological implications. *Free Radic Res.* 2003;37:121–127.

12. Landmesser U, Dikalov S, Price SR, McCann L, Fukai T, Holland SM, Mitch WE, Harrison DG. Oxidation of tetrahydrobiopterin leads to uncoupling of endothelial cell nitric oxide synthase in hypertension. *J Clin Invest.* 2003;111:1201–1209.
13. Maier W, Cosentino F, Lutolf RB, Fleisch M, Seiler C, Hess OM, Meier B, Luscher TF. Tetrahydrobiopterin improves endothelial function in patients with coronary artery disease. *J Cardiovasc Pharmacol.* 2000;35: 173–178.
14. Guzik TJ, Mussa S, Gastaldi D, Sadowski J, Ratnatunga C, Pillai R, Channon KM. Mechanisms of increased vascular superoxide production in human diabetes mellitus: role of NAD(P)H oxidase and endothelial nitric oxide synthase. *Circulation.* 2002;105:1656–1662.
15. Heitzer T, Yla-Herttuala S, Luoma J, Kurz S, Munzel T, Just H, Olschewski M, Drexler H. Cigarette smoking potentiates endothelial dysfunction of forearm resistance vessels in patients with hypercholesterolemia. Role of oxidized LDL. *Circulation.* 1996;93:1346–1353.
16. Alp NJ, Channon KM. Regulation of endothelial nitric oxide synthase by tetrahydrobiopterin in vascular disease. *Arterioscler Thromb Vasc Biol.* 2004;24:413–420.
17. Vasquez-Vivar J, Whitsett J, Martasek P, Hogg N, Kalyanaraman B. Reaction of tetrahydrobiopterin with superoxide: EPR-kinetic analysis and characterization of the pteridine radical. *Free Radic Biol Med.* 2001; 31:975–985.
18. Zheng J-S, Yang X-Q, Lookingland KJ, Fink GD, Hesslinger C, Kapatos G, Kovesdi I, Chen AF. Gene transfer of human guanosine 5′-triphosphate cyclohydrolase I restores vascular tetrahydrobiopterin level and endothelial function in low renin hypertension. *Circulation.* 2003;108:1238–1245.
19. Laursen JB, Somers M, Kurz S, McCann L, Warnholtz A, Freeman BA, Tarpey M, Fukai T, Harrison DG. Endothelial regulation of vasomotion in apoE-deficient mice: implications for interactions between peroxynitrite and tetrahydrobiopterin. *Circulation.* 2001;103:1282–1288.
20. Kuzkaya N, Weissmann N, Harrison DG, Dikalov S. Interactions of peroxynitrite, tetrahydrobiopterin, ascorbic acid, and thiols: implications for uncoupling endothelial nitric-oxide synthase. *J Biol Chem.* 2003;278: 22546–22554.
21. Vasquez-Vivar J, Martasek P, Whitsett J, Joseph J, Kalyanaraman B. The ratio between tetrahydrobiopterin and oxidized tetrahydrobiopterin analogues controls superoxide release from endothelial nitric oxide synthase: an EPR spin trapping study. *Biochem J.* 2002;362:733–739.
22. Vasquez-Vivar J, Martasek P, Kalyanaraman B. Superoxide generation from nitric oxide synthase: role of cofactors and protein interaction. In: *Biological Magnetic Resonance.* Boston, Mass: Kluwer Academic Publishers; 2005:75–91.
23. Rodriguez-Crespo I, Gerber NC, Ortiz de Montellano PR. Endothelial nitric-oxide synthase. Expression in *Escherichia coli*, spectroscopic characterization, and role of tetrahydrobiopterin in dimer formation. *J Biol Chem.* 1996;271:11462–11467.
24. Alp NJ, Mussa S, Khoo J, Guzik TJ, Cai S, Jefferson A, Rockett KA, Channon KM. Tetrahydrobiopterin-dependent preservation of nitric oxide-mediated endothelial function in diabetes by targeted transgenic GTP-cyclohydrolase I overexpression. *J Clin Invest.* 2003;112:725–735.
25. Ohashi Y, Kawashima S, Hirata K, Yamashita T, Ishida T, Inoue N, Sakoda T, Kurihara H, Yazaki Y, Yokoyama M. Hypotension and reduced nitric oxide-elicited vasorelaxation in transgenic mice overexpressing endothelial nitric oxide synthase. *J Clin Invest.* 1998;102: 2061–2071.
26. Alp NJ, McAteer MA, Khoo J, Choudhury RP, Channon KM. Increased endothelial tetrahydrobiopterin synthesis by targeted transgenic GTP-cyclohydrolase I overexpression reduces endothelial dysfunction and atherosclerosis in ApoE-knockout mice. *Arterioscler Thromb Vasc Biol.* 2004;24:445–450.
27. Klatt P, Schmidt K, Lehner D, Glatter O, Bachinger HP, Mayer B. Structural analysis of porcine brain nitric oxide synthase reveals a role for tetrahydrobiopterin and L-arginine in the formation of an SDS- resistant dimer. *EMBO J.* 1995;14:3687–3695.
28. Cai S, Alp NJ, Mc Donald D, Canevari L, Heales S, Channon KM. GTP cyclohydrolase I gene transfer augments intracellular tetrahydrobiopterin in human endothelial cells: effects on nitric oxide synthase activity, protein levels and dimerization. *Cardiovasc Res.* 2002;55:838–849.
29. Rockett KA, Brookes R, Udalova I, Vidal V, Hill AV, Kwiatkowski D. 1,25-Dihydroxyvitamin D3 induces nitric oxide synthase and suppresses growth of Mycobacterium tuberculosis in a human macrophage-like cell line. *Infect Immun.* 1998;66:5314–5321.
30. Kleschyov AL, Munzel T. Advanced spin trapping of vascular nitric oxide using colloid iron diethyldithiocarbamate. *Methods Enzymol.* 2002; 359:42–51.
31. Bendall JK, Heymes C, Wright TJ, Wheatcroft S, Grieve DJ, Shah AM, Cave AC. Strain-dependent variation in vascular responses to nitric oxide in the isolated murine heart. *J Mol Cell Cardiol.* 2002;34:1325–1333.
32. Skatchkov MP, Sperling D, Hink U, Mulsch A, Harrison DG, Sindermann I, Meinertz T, Munzel T. Validation of lucigenin as a chemiluminescent probe to monitor vascular superoxide as well as basal vascular nitric oxide production. *Biochem Biophys Res Commun.* 1999;254:319–324.
33. Khan SA, Lee K, Minhas KM, Gonzalez DR, Raju SVY, Tejani AD, Li D, Berkowitz DE, Hare JM. Neuronal nitric oxide synthase negatively regulates xanthine oxidoreductase inhibition of cardiac excitation-contraction coupling. *Proc Natl Acad Sci U S A.* 2004;101:15944–15948.
34. Channon KM, Qian HS, Neplioueva V, Blazing MA, Olmez E, Shetty GA, Youngblood SA, Stamler JS, George SE. In vivo gene transfer of nitric oxide synthase enhances vasomotor function in carotid arteries from normal and cholesterol-fed rabbits. *Circulation.* 1998;98:1905–1911.
35. Kawashima S, Yamashita T, Ozaki M, Ohashi Y, Azumi H, Inoue N, Hirata K-i, Hayashi Y, Itoh H, Yokoyama M. Endothelial NO synthase overexpression inhibits lesion formation in mouse model of vascular remodeling. *Arterioscler Thromb Vasc Biol.* 2001;21:201–207.
36. Tzeng E, Billiar TR, Robbins PD, Loftus M, Stuehr DJ. Expression of human inducible nitric oxide synthase in a tetrahydrobiopterin (H4B)-deficient cell line—H4B promotes assembly of enzyme subunits into an active enzyme. *Proc Natl Acad Sci U S A.* 1995;92:11771–11775.
37. Wever RMF, van Dam T, van Rijn HJ, de Groot F, Rabelink TJ. Tetrahydrobiopterin regulates superoxide and nitric oxide generation by recombinant endothelial nitric oxide synthase. *Biochem Biophys Res Commun.* 1997;237:340–344.

Available online at www.sciencedirect.com

SCIENCE DIRECT®

Life Sciences 76 (2004) 281–292

Life Sciences

www.elsevier.com/locate/lifescie

Pharmacokinetic and pharmacodynamic interactions between simvastatin and diltiazem in patients with hypercholesterolemia and hypertension

Hiroshi Watanabe[a,*], Kazuhiro Kosuge[a], Shinichiro Nishio[a], Hiroshi Yamada[a], Shinya Uchida[a], Hiroshi Satoh[b], Hideharu Hayashi[b], Takashi Ishizaki[c], Kyoichi Ohashi[a]

[a]*Department of Clinical Pharmacology and Therapeutics, Hamamatsu University School of Medicine, 1-20-1 Handayama, Hamamatsu 431-3192, Japan*

[b]*Department of Internal Medicine III, Hamamatsu University School of Medicine, Hamamatsu 431-3192, Japan*

[c]*Department of Pharmacology and Therapeutics, Graduate School of Clinical Pharmacy, Kumamoto University, Kumamoto 860-8555, Japan*

Received 30 April 2004; accepted 14 June 2004

Abstract

Pharmacokinetic and pharmacodynamic interactions between simvastatin, a 3-hydroxy-3-methylglutaryl coenzyme A (HMG-CoA) reductase inhibitor, and diltiazem, a calcium antagonist, were investigated in 7 male and 4 female patients with hypercholesterolemia and hypertension. The patients were given, for one in a three consecutive 4-week periods, oral simvastatin (5 mg/day), oral simvastatin (5 mg/day) combined with diltiazem (90 mg/day), and then oral diltiazem (90 mg/day), respectively. The area under the plasma concentration versus time curve up to 6 hours post-dose (AUC_{0-6h}) and maximum plasma concentrations (Cmax) of the drugs, serum lipid profiles, blood pressures and liver functions were assessed on the last day of each of the three 4-week periods. After the combined treatment period, Cmax of HMG-CoA reductase inhibitor was elevated from 7.8 ± 2.6 ng/ml to 15.4 ± 7.9 ng/ml ($P < 0.01$) and AUC_{0-6h} from 21.7 ± 4.9 ng·hr/ml to 43.3 ± 23.4 ng·hr/ml ($P < 0.01$), while Cmax of diltiazem was decreased from 74.2 ± 36.4 ng/ml to 58.6 ± 18.9 ng/ml ($P < 0.05$) and its AUC_{0-6h} from 365 ± 153 ng·hr/ml to 287 ± 113 ng·hr/ml ($P < 0.01$). Compared to simvastatin monotherapy, combined treatment further reduced LDL-cholesterol levels by 9%, from 129 ± 16 mg/dl to 119 ± 17 mg/dl ($P < 0.05$). No adverse events were observed throughout the study. These apparent pharmacokinetic interactions, namely the increase of HMG-CoA reductase inhibitor concentration by diltiazem

* Corresponding author. Tel.: +81 53 435 2385; fax: +81 53 435 2384.
E-mail address: hwat@hama-med.ac.jp (H. Watanabe).

doi:10.1016/j.lfs.2004.06.022

and the decrease of diltiazem concentration by simvastatin, enhance the cholesterol-lowering effects of simvastatin during combined treatment.

Keywords: HMG-CoA reductase inhibitor; Simvastatin; Diltiazem; Pharmacokinetic interaction; Pharmacodynamic interaction

Introduction

Control of hypercholesterolemia is of prime importance for the primary and secondary prevention of coronary artery disease (CAD) (Gould et al., 1995; Tonkin, 1995; Shepherd, 1998). Currently, 3-hydroxy-3-methylglutaryl-coenzyme A (HMG-CoA) reductase inhibitors are the first-line therapy for patients with elevated serum low-density lipoprotein (LDL)-cholesterol (Gotto, 1998; Wood, 2001). Among the HMG Co-A reductase inhibitors, simvastatin is widely used and has been shown to reduce morbidity and mortality from CAD (The Scandinavian Simvastatin Survival Study, 1994). Simvastatin is an inactive lactone pro-drug that is hydrolysed by esterases to simvastatin acid, the active competitive inhibitor of HMG-CoA reductase (Vickers et al., 1990, 1990; Prueksaritanont et al., 1997). Since HMG-CoA reductase is responsible for the conversion of HMG-CoA to mevalonic acid, the rate-limiting step in the hepatic cholesterol biosynthesis, the inhibition of HMG-CoA reductase lowers serum cholesterol levels (Goldstein and Brown, 1990). Although cytochrome P450 (CYP) is not involved in the conversion of simvastatin to simvastatin acid, the oxidative metabolism of simvastatin to the metabolites, 3′,5′-dihydrodiol, 3′-hydroxy and 6′-exomethylene, is mainly mediated by CYP3A4 (Vickers et al., 1990, 1990; Prueksaritanont et al., 1997). In a crossover study in healthy volunteers (Neuvonen et al., 1998), the areas under the plasma concentration versus time curves (AUCs) of simvastatin and simvastatin acid after a single oral dose of simvastatin were increased 10-fold and 19-fold, respectively, following 4 days of treatment with 200 mg/day itraconazole, an agent that has been shown to increase the plasma concentrations and half-lives of many drugs metabolized by CYP3A4 by inhibiting the enzyme (Kivistö et al., 1997; Wang et al., 1999).

Hypercholesterolemia is often accompanied by hypertension, an associated risk factor for CAD (Gould et al., 1995; Gotto, 1998; Wood, 2001). The calcium antagonist diltiazem is effective for the management of hypertension, supraventricular arrhythmias and angina pectoris (Chaffman and Brogden, 1985; Hansson et al., 2000; Nakagawa and Ishizaki, 2000), and is often prescribed in association with lipid-lowering agents like simvastatin (The Scandinavian Simvastatin Survival Study, 1994; Gotto, 1998; Wood, 2001). Diltiazem is extensively metabolized in the liver, primarily by deacetylation and demethylation by CYP3A4 into a host metabolite, N-desmethyl-diltiazem, which, together with diltiazem, in turn selectively inhibits CYP3A4, but not CYP1A2, CYP2C9, or CYP2E1 (Sutton et al., 1997; Jones et al., 1999). Accordingly, pharmacokinetic and pharmacodynamic interactions may theoretically happen upon co-administration of diltiazem and a drug metabolized by CYP3A4 like simvastatin.

Indeed, combined treatment of diltiazem and simvastatin has been shown to cause a 5-fold increase in the AUC of simvastatin (Mousa et al., 2000). Lovastatin, which is pharmacokinetically similar to simvastatin, also interacts with diltiazem (Azie et al., 1998). A recent retrospective analysis shows that patients who had taken both simvastatin and diltiazem needed lower doses of simvastatin to achieve

the recommended reduction in serum cholesterol (Yeo et al., 1999), suggesting a pharmacokinetically-driven pharmacodynamic interaction between the two drugs. However, steady state bi-directional pharmacokinetic and pharmacodinamic interactions between simvastatin and diltiazem has not been prospectively evaluated. In this study we prospectively studied the pharmacokinetic and pharmacodynamic interactions between simvastatin and diltiazem in patients with hypercholesterolemia and hypertension.

Methods

Subjects

Enrolled were 7 male and 4 female patients (age: 62.0 ± 7.5 years; body weight: 62.6 ± 5.4 kg, mean ± S.D.) with hypercholesterolemia and hypertension who had taken simvastatin (5 mg/day) and the angiotensin-converting enzyme inhibitor enalapril (5 mg/day) for more than 3 months and had reached the plateau control (Table 1). Inclusion criteria were: age of at least 18 years, basal total cholesterol or LDL-cholesterol levels greater than 220 mg/dl or 140 mg/dl, respectively, and systolic blood pressure (BP) or diastolic BP levels greater than 140 mmHg or 90 mmHg, respectively, without medication. Before the start of any lipid-lowering and antihypertensive therapy, basal total cholesterol levels were 249 ± 28 mg/dl; LDL-cholesterol, 166 ± 23 mg/dl; systolic BP, 151 ± 29 mm Hg; and diastolic BP, 88 ± 11 mm Hg. The subjects had no history of hepatic or renal disease. At the end of the pre-trial phase with simvastatin (5 mg/day) and enalapril (5 mg/day) for more than 3 months, the average total cholesterol level was 207 ± 23 mg/dl; LDL-cholesterol, 129 ± 15 mg/dl; systolic BP, 142 ± 22 mm Hg; and diastolic BP, 84 ± 12 mm Hg.

Table 1
Patient demographics and basic medical data (mean ± S.D.)

Age (y)	62.0 ± 7.5
Sex (M/F)	7/4
Body weight (kg)	62.6 ± 5.4
Serum creatinine (mg/dl)	0.72 ± 0.19
AST (IU/l)	21.4 ± 3.8
ALT (IU/l)	20.0 ± 9.3
Creatine kinase (IU/l)	109 ± 48
Total cholesterol (mg/dl)	249 ± 28
LDL-cholesterol (mg/dl)	166 ± 23
HDL-cholesterol (mg/dl)	50 ± 10
Triglyceride (mg/dl)	168 ± 82
Systolic BP (mmHg)	151 ± 29
Diastolic BP (mmHg)	88 ± 11
Heart rate (beats/min)	72 ± 10

AST, aspartate aminotransferase; ALT, alanine aminotransferase; LDL, low-density lipoprotein; HDL, high-density lipoprotein; BP, blood pressure.

Study design

This was a three-phase fixed-order design study: (1) administration of oral simvastatin (5 mg/day) for 4 weeks, (2) co-administration of oral diltiazem (30 mg three times a day) and simvastatin (5 mg/day) for 4 weeks, and (3) administration of oral diltiazem (90 mg/day) alone for another 4 weeks. The AUC up to 6 hours post-dose (AUC_{0-6h}) and Cmax of the drugs, serum lipid profiles and liver function were evaluated, as specified below. No drug other than simvastatin and/or diltiazem was taken during the study period. Patients who developed symptoms due to withdrawal of lipid-lowering medication or whose systolic BP or diastolic BP respectively exceeded 180 mmHg or 110 mmHg following discontinuation of antihypertensive therapy were withdrawn from the study and appropriate therapy re-established. The study protocol, consent forms, and volunteer information documents were approved by Hamamatsu University School of Medicine Independent Review Board. All subjects provided written informed consent before participating in the trial.

Blood sampling

Blood samples were obtained on the last day of each of the three 4-week periods. After an overnight fast, a pre-dosing venous blood sample was taken, and then simvastatin (5 mg) and/or diltiazem (30 mg) was/were given. All patients drank a glass of water after swallowing the tablets. Blood samples were then taken 2, 3, 4 and 6 hours later. Standardized breakfast and lunch were served 2 and 4 hours after drug intake. Plasma was separated within 30 minutes and stored at −70 °C until analysis.

Blood pressure measurement

On the last day of each trial periods, systolic BP and diastolic BP were measured twice each using an automatic electronic sphygmomanometer (BP-103i II, Nippon Colin, Komaki, Japan) at the sitting position before and 2, 3, 4 and 6 hours after the administration of the drug(s).

Determination of diltiazem concentration

Diltiazem concentrations were measured by an HPLC assay with an ultraviolet detection, as described by Abernethy et al. (1985). Diltiazem was resolved from the internal standard desipramine with a mobile phase of 0.06 mol/l acetate buffer/acetonitrile/methanol (58:37:5) that contained 5 mmol/l heptane sulfonic acid and glacial acetic acid to adjust pH to 6.4. A reversed-phase C_{18}μBondapak column (30 cm×3.9 mm, Waters Chromatography, Milford, MA) was eluted at 1.8 ml/min and detection was performed by ultraviolet absorbance at 254 nm. The calibration range was 5–300 ng/ml. The intra-day and inter-day coefficients of variation were less than 9%.

Determination of simvastatin HMG-CoA reductase inhibitor concentrations

HMG-CoA reductase inhibitor concentrations were determined as previously described (Arnadottir et al., 1993). An equal volume of methanol was added to the plasma samples and the mixtures were vortexed thoroughly, kept on ice for 10 minutes and centrifuged. Fifty microliters of the supernatants were dried in an evaporator (SpeedVac, Savant Instr. Farmingdale, NY). The reaction mixture (96 μl) was added

directly to the dried residues to make a final volume of 100 μl containing 0.1 M KPO_4 (pH 7.4), 10 mM 1, 4-dithiothreitol (DTT), 0.2 mM $NADH^-$ (made fresh daily), 5 mM glucose-6-phosphate, 1.4 U/ml glucose-6-phosphate dehydrogenase and 1 mg/ml bovine serum albumin. The reaction mixture was incubated for 5 minutes at 37 °C and soluble rat liver HMG-CoA reductase was added to 2 μl buffer A: 0.04 M KPO_4 (pH 7.4), 0.05 M KCl, 0.1 M sucrose, 0.03 M ethylenediaminetetraacetic acid (EDTA) and 0.01 M DTT (added immediately before use). The mixture was incubated at 37 °C for 5 minutes in the presence of the inhibitor-containing plasma sample. The reaction was then started with 2 μl of 1.25 mg/ml HMG-CoA containing 17.5 μCi/ml glutaryl-3-[^{14}C]-HMG-CoA. After an additional 6-minute incubation at 37 °C, 20 μl of 5 N HCl was added to lactonize the mevalonic acid formed. After 15 minutes, 3.5 ml of a 1:1 suspension of BioRad AG 1 × 8 resin (200–400 mesh) was added and the tubes (13 × 100) were thoroughly vortexed. [^{14}C]-mevalonolactone was filtered from the resin suspension through polystyrene filters (pore size 70 μm, EverGreen, Los Angeles, CA) into scintillation vials containing 15 ml of Aquasol-2 (New England Nuclear, Newton, MA) and counted on a scintillation counter. Percent inhibition was converted to the inhibitor concentration using a standard curve constructed by extracting from the control plasma containing known amounts of L-654, 969, the free acid form of simvastatin. The results were expressed as nanograms of inhibitor per milliliter of plasma. The intra-day and inter-day coefficients of variation for the HMG-CoA reductase activity assay were less than 6%.

Statistical analysis

Data were analyzed by 2-way ANOVA, a paired Student's *t* test, or Wilcoxon signed-rank test where appropriate. Differences with P values < 0.05 were considered statistically significant. All values are given as means ± S.D.

Results

Pharmacokinetic interactions between simvastatin and diltiazem

HMG-CoA reductase inhibitor concentrations after simvastatin administration with or without diltiazem are shown in Fig. 1A. HMG-CoA reductase inhibitor values for Cmax, time to Cmax (Tmax) and AUC_{0-6h} after simvastatin administration without diltiazem were 7.8 ± 2.6 ng/ml, 2.3 ± 0.5 h and 21.7 ± 4.9 ng·h/ml, respectively. Co-administration of diltiazem with simvastatin increased Cmax and AUC_{0-6h} of HMG-CoA reductase inhibitor concentrations to 15.4 ± 7.9 ng/ml ($P < 0.01$) and 43.3 ± 23.4 ng·h/ml ($P < 0.01$), respectively (Fig. 1B), but did not affect Tmax of HMG-CoA reductase inhibitor (2.3 ± 0.5 h). There was a considerable inter-individual variability in the effect of diltiazem on the levels of HMG-CoA reductase inhibitor (Fig. 1B): the AUC_{0-6h} of HMG-CoA reductase inhibitor concentration was increased by 422% in a patient and 7% in another.

Diltiazem concentrations after diltiazem administration with and without simvastatin are shown in Fig. 2A. After the last oral intake of diltiazem without simvastatin, Cmax, Tmax and AUC_{0-6h} of diltiazem were 74.2 ± 36.4 ng/ml, 3.4 ± 1.2 h and 365 ± 153 ng·h/ml, respectively. In contrast to the effects of the combined treatment on the pharmacokinetics of HMG-CoA reductase inhibitor concentrations, co-administration of simvastatin with diltiazem decreased Cmax and AUC_{0-6h} of diltiazem to 58.6 ± 18.9 ng/ml ($P < 0.05$) and 287 ± 113 ng·h/ml ($P < 0.01$), respectively, while the

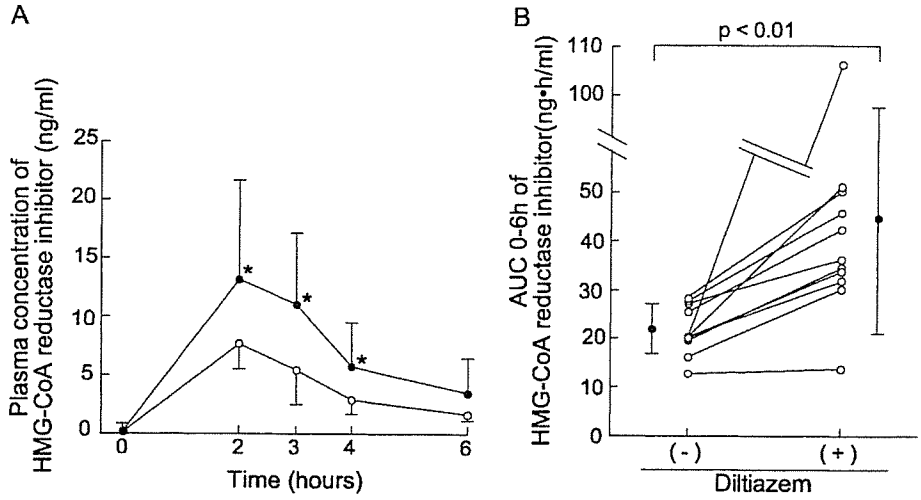

Fig. 1. Effect of diltiazem on plasma concentration and $AUC_{0\ 6h}$ of HMG-CoA reductase inhibitor. (A) Plasma concentrations of HMG-CoA reductase inhibitor observed on the last day of 4 weeks of treatment with simvastatin (5mg/day) (open circles) or combined treatment with simvastatin (5mg/day) and diltiazem (90mg/day) (closed circles). Error bars represent S.D. *Significant difference from simvastatin monotherapy ($P < 0.05$). (B) Individual $AUC_{0\ 6h}$ values for HMG-CoA reductase inhibitor (open circles) with (right) and without diltiazem (left) in the 11 patients. Closed circles with the bars indicate means ± S.D.

Tmax of diltiazem was not affected (3.1 ± 0.9 h) by simvastatin. Plasma diltiazem AUC_{0-6h} values were decreased by simvastatin in 9 of the 11 patients (Fig. 2B).

Pharmacodynamic interactions between simvastatin and diltiazem

Following 4 weeks of simvastatin monotherapy, total cholesterol, LDL-cholesterol, HDL-cholesterol, and triglyceride levels were 206 ± 26 mg/dl, 129 ± 16 mg/dl, 50 ± 10 mg/dl, and 135 ± 73 mg/dl,

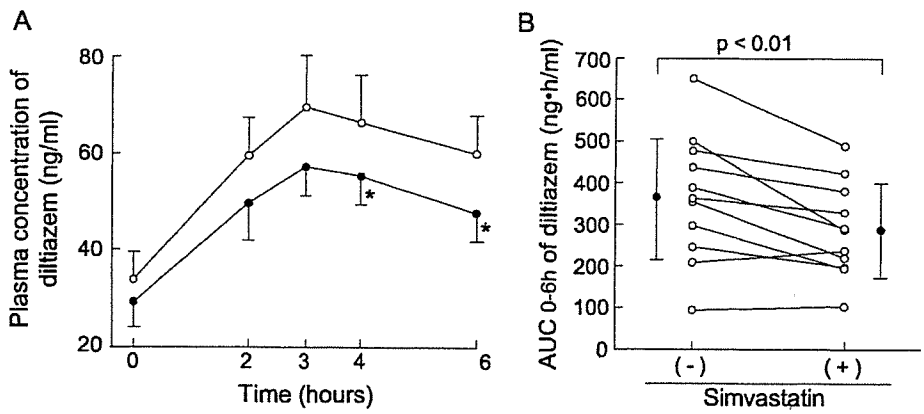

Fig. 2. Effect of simvastatin on plasma concentration and $AUC_{0\ 6h}$ of diltiazem. (A) Plasma concentrations of diltiazem observed on the last day of 4 weeks of treatment with diltiazem (open circles) or combined treatment with simvastatin and diltiazem (closed circles). *Significant difference from diltiazem monotherapy ($P < 0.05$). (B) Individual $AUC_{0\ 6h}$ values of diltiazem (open circles) with (right) and without simvastatin (left). Closed circles with the bars indicate means ± S.D.

respectively (Fig. 3A). These values were not different with those at the end of pretrial phase with simvastatin (5 mg/day) and enalapril (5 mg/day) (total cholesterol, 207 ± 23 mg/dl; LDL-cholesterol, 129 ± 15 mg/dl; HDL-cholesterol, 50 ± 10 mg/dl; triglyceride, 137 ± 68 mg/dl), suggesting that the treatment with simvastatin reached the platcau control during the pretrial phase. Co-administration of diltiazem and simvastatin further reduced the mean total and LDL-cholesterol levels to 196 ± 32 mg/dl ($P < 0.05$) (Fig. 3B) and 119 ± 17 mg/dl ($P < 0.05$), respectively, but did not influence HDL-cholesterol and triglyceride levels, which were 49 ± 11 mg/dl and 140 ± 72 mg/dl, respectively. On the other hand, after simvastatin was withdrawn during the last 4 weeks of diltiazem monotherapy, total cholesterol and LDL-cholesterol levels increased to 245 ± 33 mg/dl and 163 ± 21 mg/dl ($P < 0.01$), respectively, while HDL-cholesterol and triglyceride levels were not affected (51 ± 12 mg/dl and 157 ± 77 mg/dl, respectively).

After 4 weeks of simvastatin monotherapy, baseline systolic and diastolic BP increased from 142 ± 22 mm Hg to 152 ± 28 mm Hg ($P < 0.05$) and from 84 ± 12 mm Hg to 89 ± 10 mm Hg ($P < 0.05$), respectively, compared to baseline BP during the pre-trial phase with simvastatin and enalapril. Simvastatin did not exert any BP-lowering effect. Diltiazem decreased systolic BP from 146 ± 26 mm Hg to 124 ± 9 mm Hg and diastolic BP from 84 ± 11 mm Hg to 75 ± 6 mm Hg at 2 hours post-dose. This effect was not influenced by the combined treatment with simvastatin (baseline systolic BP, 138 ± 18 mm Hg; baseline diastolic BP, 83 ± 13 mm Hg; systolic BP at 2 hours post-dose, 129 ± 19; diastolic BP at 2 hours post-dose, 76 ± 12 mm Hg) (Fig. 4).

Serum aspartate aminotransferase (AST; normal range, 11–30 IU/l), alanine aminotransferase (ALT; normal range, 5–42 IU/l), lactate dehydrogenase (LDH; normal range, 115–208 IU/l) and creatine kinase (CK; normal range, 55–204 IU/l) levels appeared to increase, albeit without statistical significance, during the combined therapy period compared with those observed during the simvastatin monotherapy

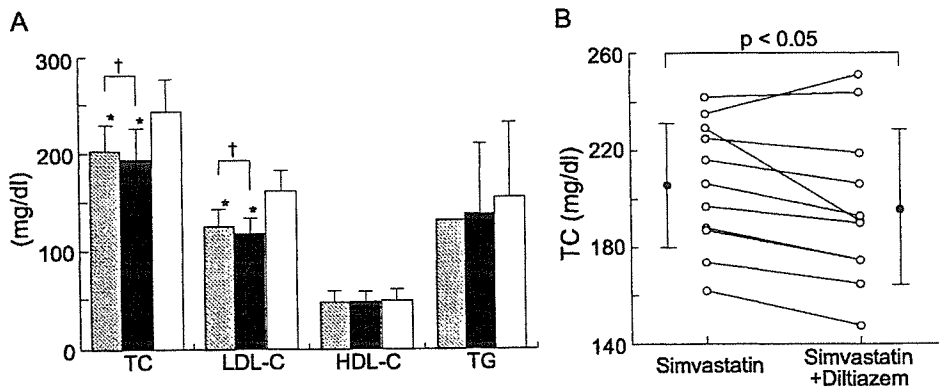

Fig. 3. Lipid profiles during simvastatin monotherapy, combined therapy with diltiazem and simvastatin, and diltiazem monotherapy. (A) Lipid profiles after 4 weeks of simvastatin monotherapy (5mg/day, hatched columns), combined treatment with simvastatin (5mg/day) and diltiazem (90mg/day) (closed columns) or diltiazem monotherapy (90mg/day, open columns). TC, total cholesterol; LDL-C, low-density lipoprotein cholesterol; HDL-C, high-density lipoprotein cholesterol and TG, triglyceride. * Significant difference from diltiazem monotherapy ($P < 0.05$). †Significant difference between simvastatin monotherapy and combined treatment with simvastatin and diltiazem ($P < 0.05$). (B) Total cholesterol levels in the 11 patients observed after 4 weeks of treatment with simvastatin (90mg/day) (left) or combined treatment with simvastatin (5mg/day) and diltiazem (90mg/day) (right). Closed circles with the bars indicate means ± S.D.

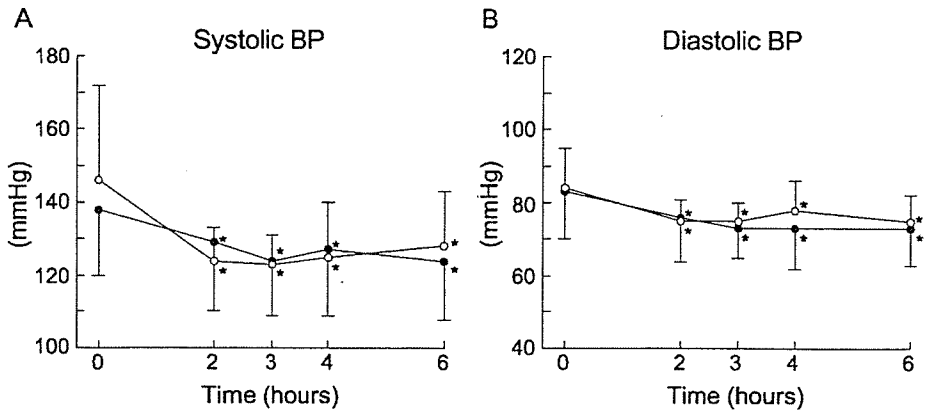

Fig. 4. Blood pressures during combined therapy with diltiazem and simvastatin, and diltiazem monotherapy. Systolic (A) and diastolic (B) BP before and 2, 3, 4 and 6 hours after an oral 30 mg dose of diltiazem with (closed circles) or without (open circles) simvastatin following 4 weeks of treatment with diltiazem alone (90mg/day) (open circles) or combined treatment with simvastatin (5mg/day) and diltiazem (90mg/day) (closed circles). * Significant difference from BP at 0 h ($P < 0.05$). Data are expressed as means ± S.D.

period: AST, 23.4 ± 4.3 IU/l vs. 21.3 ± 5.1 IU/l, ALT, 22.1 ± 5.6 IU/l vs. 18.9 ± 5.6 IU/l, LDH, 196 ± 42 IU/l vs. 187 ± 32 IU/l, and CK 142 ± 111 IU/l vs. 107 ± 45 IU/l, respectively.

Discussion

Simvastatin and diltiazem are often prescribed together for the treatment of hypercholesterolemia in patients with hypertension and/or angina pectoris (Gould et al., 1995; Gotto, 1998; Wood, 2001). In the Scandinavian Simvastatin Survival Study (4S) (1994), which demonstrated a reduction in nonfatal myocardial infarction, cardiovascular death, and total mortality by simvastatin treatment in patients with angina pectoris or previous myocardial infarction, more than 30% of the study population were treated with calcium antagonists including diltiazem. The efficacy and safety profiles of simvastatin and diltiazem are widely accepted (Chaffman and Brogden, 1985; The Scandinavian Simvastatin Survival Study, 1994; Hansson et al., 2000). The effect of diltiazem on the pharmacokinetics of simvastatin has been previously described, such that the Cmax and AUC of simvastatin after a single 20 mg oral dose of simvastatin increased by 3.6-fold and 5-fold, respectively, after 2 weeks of treatment with 120 mg diltiazem twice a day (Mousa et al., 2000). However, bi-directional pharmacokinetic interactions and the potential pharmacodynamic impact have not been prospectively studied.

Our prospective study demonstrates that long-term and low-dose co-administration of diltiazem and simvastatin results in two-fold increase of Cmax and AUC of HMG-CoA reductase inhibitor, which is accompanied by enhanced cholesterol-lowering effect of simvastatin in patients with hypercholesterolemia and hypertension. Interestingly, in contrast to the effect on the pharmacokinetics of simvastatin, the co-administration of simvastatin with diltiazem decreased the Cmax and AUC of diltiazem without affecting its BP-lowering effects.

These results are consistent with a retrospective study demonstrating that simvastatin caused a 33.3% cholesterol reduction in patients using diltiazem compared with 24.7% in those not using diltiazem (Yeo

et al., 1999). It has also been reported that doubling the dose of simvastatin further reduces serum cholesterol by an average of 5% (Roberts, 1997). This is compatible with our finding that a two-fold increase in the Cmax and AUC of HMG-CoA reductase inhibitor by co-administration of diltiazem with simvastatin was accompanied by a further 5% reduction in total cholesterol level. The results of our study suggest that patients who require both simvastatin and diltiazem may need a lower dose of simvastatin than when simvastatin is prescribed alone to achieve the desired reduction in total and LDL-cholesterol levels.

The mechanism underlying the decrease in the AUC of diltiazem by the combined therapy with simvastatin remains unknown. Diltiazem is extensively metabolized in the liver into its host metabolites, primarily by deacetylation and demethylation by CYP3A4 in vitro and in vivo (Chaffman and Brogden, 1985; Pichard et al., 1990; Sutton et al., 1997; Jones et al., 1999; Nakagawa and Ishizaki, 2000; Yeo and Yeo, 2001; Kosuge et al., 2001), and probably in part by CYP2C8/9 (Sutton et al., 1997). In addition, diltiazem has been shown to increase the metabolic ratio of debrisoquine (Sakai et al., 1991), suggesting a possible interference with CYP2D6 (Molden et al., 2002). It is possible that the relevant enzyme activity to metabolize diltiazem or its metabolite(s) might be induced by themselves. Alternatively, simvastatin and/or its metabolite(s) might enhance the activity of enzyme(s) involved in the metabolism of diltiazem after the long term coadministration. Although the Cmax and AUC of diltiazem were decreased by simvastatin, blood pressure-lowering effect of diltiazem was not influenced by simvastatin. Heart rate of the patients during combined treatment with simvastatin did not differ from that during the diltiazem monotherapy period: 70 ± 10 beats/min vs. 68 ± 7 beats/min, respectively. It is likely that the pharmacokinetic interaction such as the 21% reduction in both the Cmax and AUC of diltiazem was not sufficient to alter pharmacodynamic response. However, we cannot exclude the possibility that the power was not enough to detect the pharmacodynamic differences. Further investigation is required to clarify the pharmacodynamic impact on blood pressure and the mechanism responsible for the changes in the pharmacokinetic behavior of diltiazem by the combined treatment with simvastatin.

The combined therapy increased the AUC of HMG-CoA reductase inhibitor by as much as 422% in one patient and as little as 7 % in another, suggesting a considerable inter-individual variability in the effect of diltiazem on the levels of HMG-CoA reductase inhibitor (Fig. 1B). However, this pharmacokinetic variation did not account for the differences in the pharmacodynamic responses to simvastatin (correlation coefficient: $r = 0.106$, not significant) (Fig. 5A). On the other hand, there was a significant correlation between the AUC of diltiazem and the AUC of HMG-CoA reductase inhibitor ($r = 0.73$, $P < 0.05$) (Fig. 5B). For example, one patient showing the lowest value of the AUC of diltiazem showed the lowest value for the AUC of HMG-CoA reductase inhibitor, suggesting that this patient might be an individual with a high CYP3A4 activity. These findings taken together strongly suggest that simvastatin and diltiazem could be metabolized, at least in part, through a common or shared pathway.

Simvastatin is generally well tolerated and causes few subjective side-effects during chronic treatment, however, rhabdomyolysis is a rare side effect of this HMG-CoA reductase inhibitor that appears to be dose-related. The doses of simvastatin (5 mg/day) and diltiazem (90 mg/day) used in this study are lower than those recommended in Western countries, because these doses are common and approved in the Japanese formulary and have been shown to be sufficient to treat Japanese patients at the clinical practice (Matsuzaki et al., 2002). It is noteworthy that the pharmacokinetic and pharmacodynamic interactions take place even at the lower doses. Furthermore, the levels of AST, ALT, LDH and CK appeared to increase during the combined therapy with simvastatin and diltiazem compared to the